Interfacial Water Structure and Effects of Mg^{2+} and Ca^{2+} Binding to the COOH Headgroup of a Palmitic Acid Monolayer Studied by Sum Frequency Spectroscopy

Cheng Y. Tang, Zishuai Huang, and Heather C. Allen*

The Ohio State University, Department of Chemistry, 100 West 18th Avenue, Columbus, Ohio 43210, United States

Received: July 6, 2010; Revised Manuscript Received: November 25, 2010

The interfacial hydrogen-bonding network that uniquely exists in between a palmitic acid (PA) monolayer and the underneath surface water molecules was studied using vibrational sum frequency generation (VSFG) spectroscopy. Perturbations due to cation binding of Mg^{2+} and Ca^{2+} were identified. The polar ordering of the interfacial water molecules under the influence of the surface field of dissociated PA headgroups was observed. Only a fraction of PA molecules are deprotonated at the air/water interface with a neat water subphase, yet the submonolayer concentration of negatively charged PA headgroups induces considerable polar ordering on the interfacial water molecules relative to the neat water surface without the PA film. Upon addition of calcium and magnesium chloride salts to the subphase of the PA monolayer, the extent of polar ordering of the interfacial water molecules was reduced. Ca^{2+} was observed to have the greater impact on the interfacial hydrogen-bonding network relative to Mg^{2+}, consistent with the greater binding affinity of Ca^{2+} toward the carboxylate group relative to Mg^{2+} and thereby modifying the interfacial charge. At high-salt concentrations, the already disrupted hydrogen-bonding network reorganizes and reverts to its original hydrogen-bonding structure as that which appeared at the neat salt solution surface without a PA monolayer.

Introduction

Water is essential to life and is implicated in many biological processes in addition to atmospheric aerosol processing. Although much effort has been expended on understanding of the physicochemical nature of water in these processes, many questions remain to be addressed. Incomplete is our understanding of the biological functions of water at a molecular scale and the nonbulk-like behavior of vicinal water molecules adjacent to biological macromolecules such as protein surfaces. For instance, it is found that vicinal water molecules differ in density, specific heat, viscosity, and other physical properties in comparison to the bulk water;[1] furthermore, the dynamic nature of these water molecules is versatile enough to exhibit an expansion on the time scale of an order to match the slow dynamics of macromolecules in the course of changing conformations, namely, protein folding.[2,3] Intrinsically, interfacial water structure is different from the bulk.

Langmuir monolayers have been studied extensively in the past and continue to attract more interest in scientific investigations. For instance, Langmuir monolayers have been commonly used as empirical paradigms that mimic biological membranes and biomimetic material surfaces.[4] In addition, Langmuir monolayers have been used as proxies for organic-coated atmospheric marine and continental aerosols.[5,6] Of great importance in past studies is to understand physicochemical properties of Langmuir monolayers that encompass molecular structure,[7,8] molecular assemblies,[9] film rheology,[10] complex aggregates,[11,12] and molecular interactions.[13,14] The advantage of using Langmuir monolayers as model systems for real biological and atmospheric aerosol processes could best reflect upon realizations of easy manipulation of experimental parameters that would otherwise be difficult to achieve in bulk phase or at other interfaces. These include surface pressure, molecular coverage, and film morphology.

More importantly, studying the hydrogen-bonding structure of surface water molecules residing underneath a Langmuir monolayer could provide a more in-depth molecular-level understanding of water structure and molecular interaction of water molecules with polar headgroups of amphiphilic molecules. With incorporation of divalent cations such as Mg^{2+} and Ca^{2+} in the aqueous subphase, the dynamic nature of the interfacial hydrogen-bonding network due to the presence of the inorganic cations (and anions) becomes more pertinent to the real biological and atmospheric aerosol systems. Ultimately, studying more real and complex systems may help to make predictions regarding surface phenomena that are commonly found at both biological and atmospheric aerosol interfaces.

To date, development of methodologies in surface science has advanced considerably. For example, traditional techniques used to characterize Langmuir monolayers include compression isotherms and surface potential measurements from which phase information and surface potential variation could be monitored.[15,16] As part of structural investigations, domain structures have been studied using fluorescence and Brewster angle microscopes;[17,18] studies of molecular orientation and film packing configurations using X-ray reflection and diffraction techniques and the neutron reflection technique have been routinely implemented in laboratories.[7,8] In addition, infrared reflection and absorption spectroscopy (IRRAS) and nonlinear optical spectroscopy have also been used in molecular identification and structural investigations of Langmuir monolayers.[19−22] Among these techniques, the nonlinear optical spectroscopic techniques, namely, vibrational sum frequency generation (VSFG) spectroscopy is deemed ideal for studying interfacial hydrogen-bonded water structure at interfaces, especially at buried interfaces.[23−36] However, other techniques have also been applied in similar studies to interrogate water and headgroup

* To whom correspondence should be addressed.

10.1021/jp1062447
Published on Web 12/15/2010

interactions. As an example, based on an X-ray diffraction study Dutta and co-workers determined that beneath an ordered and condensed heneicosanoic acid (C_{21}) monolayer, an ordered inorganic layer exists in the sublayer as a result of forming a superlattice structure between Mg^{2+} and the headgroup.[37] By using the same technique, Tikhonov et al. proposed that water molecules could penetrate into alkanol monolayers with a stoichiometric ratio of 3:1 of alkanol over water at the alkanol/hexane interface.[38] On the other hand, Liu et al. studied metal coordination with carboxylate groups in monolayers of Schiff bases using IRRAS; however, no discussion was given to elaborate the observed ~3600 cm^{-1} O−H band that corresponded to the hydrogen-bonded headgroups except stating a correlation between this band intensity with film thickness.[39] In a theoretical study, Ivanova et al. simulated molecular interactions between water molecules and hydrophilic headgroups of commonly found surfactant molecules using ab initio calculations and concluded that the molecular dipole moment in the interfacial region is affected by the local environment.[40]

VSFG is specific to anisotropic media such as interfaces separating two isotropic bulk media under the dipole approximation. Combining this surface specificity and its submonolayer sensitivity, VSFG is a powerful tool in probing interfacial hydrogen-bonded water structure. Most recently, phase-sensitive VSFG (PS-VSFG) spectroscopic studies provide a direct probe of interfacial water orientation.[41−43] To date, conventional (as opposed to phase-sensitive) VSFG has been applied in studies at the air/liquid, liquid/liquid, and liquid/solid interfaces. For example, ionic perturbations on the interfacial hydrogen-bonded water structure at the air/liquid interface have been systematically studied by a number of research groups, which covered an extensive list of both anions and cations species.[28,44−50] Furthermore, interfacial water structures at the hydrophilic and hydrophobic interfaces were also extensively studied and compared.[51−54] The objectives were not only placed on the interface effects, but also on the adsorption effects owing to a complex array of intermolecular interaction forces. Recently, the absolute phase of the O−H oscillator of interfacial hydrogen-bonded water molecules was experimentally determined using PS-VSFG; by varying surface electric charge from positive to negative, interfacial water molecules were shown to exhibit flip-flop characteristics.[42] Considering the nature of hydrogen-bonding network underneath a fatty acid monolayer, only a limited number of VSFG studies have been attempted in the recent past. Miranda et al. were the first to study the hydrogen-bonding network that exists at the fatty acid monolayer−water interface.[52] By varying pH values from acidic to basic in the subphase, they identified a rich hydrogen-bonding network between surface water molecules and hexacosanoic (C_{26}) acid headgroups. However, phase and ionic binding effects were not addressed. On the other hand, Cremer and co-workers were interested in the effects induced by the divalent cations (Mg^{2+} and Zn^{2+}) binding to the dissociated carboxylic headgroups of eicosanoic (C_{20}) acid monolayers on the interfacial hydrogen-bonded water structure.[51] In that study, dilute inorganic salt concentrations were considered. In simulating biological processes, studying near neutral pH is essential in addition to inclusion of biologically relevant cation species.

Here, we studied the molecular structure of interfacial hydrogen-bonding network underneath a palmitic acid (C_{16}; PA) monolayer under the influence of two salts $MgCl_2$ and $CaCl_2$ studying the Mg^{2+} and Ca^{2+} binding effects at a near neutral pH (6.0). By varying the cation concentrations, surface water restructuring mechanisms were identified due to the surface charge neutralization effect. We found that at lower concentrations, surface neutralization is the prominent effect; however, at higher concentrations, post reaching the point zero charge (PZC) transition of the fatty acid monolayer, the already disrupted hydrogen-bonding network reorganizes and reverts to the original water structure as that which is observed at the neat salt solution interface for both cations.

Experimental Section

Materials. Palmitic acid (>99%, Sigma-Aldrich) was used to prepare solutions at ~1.5 mM by dissolving in spectroscopic-grade chloroform (>99.9, Sigma-Aldrich). Magnesium chloride hexahydrate (certified ACS, 99%, Fisher Scientific) and calcium chloride dihydrate (USP/FCC, 99%, Fisher Scientific) were used to prepare stock solutions by dissolving in deionized water (18.2 MΩ·cm resistivity) from a Barnstead Nanopure system at pH of 6.0.

Stock solutions were filtered twice to eliminate potential organic contaminants using a Whatman Carbon-Cap activated carbon filter. The concentrations of the filtered stock solutions were standardized based on the Mohr titration technique[55] in which silver nitrate (reagent grade, Fisher Scientific) and potassium chromate (99.5%, E.M. Science) were used as a titrant and an indicator, respectively. 0.1, 0.3, 1.5, and 1.8 M (molarity) inorganic salt solutions used in this study were prepared by dilution, and 2.6 M Mg^{2+} was prepared by evaporation of the stock solution in a water bath. All solutions were conditioned at room temperature (23 ± 1 °C) over 24 h before use. To confirm solutions to be devoid of any possible organic contaminant, VSFG spectra were shown to be absent of C−H stretching intensities in the spectral window of 2800−3000 cm^{-1}.

Methods. Monolayers were spread over the various solutions in Petri-dishes by adding dropwise using a Hamilton syringe a predetermined number of PA molecules in chloroform. Ten minutes were allowed to elapse for monolayer stabilization prior to VSFG spectral acquisition. SFG acquisitions were attained directly after this elapsed time. The monolayers of PA on neat water and the salt solutions were able to attain a highly ordered condensed phase at mean molecular area (MMA) coverage of ~21 $Å^2$/molecule as confirmed by VSFG probing the PA molecules (data not shown).

Broad Bandwidth Sum Frequency Generation Instrumentation. The broad bandwidth VSFG spectrometer setup has been described elsewhere.[56−58] Here, additional details specific to this experiment are discussed. On average, the spectral bandwidth (fwhm) of the broadband infrared beam is ~450 cm^{-1} when optimized for the bandwidth while being centered at ~3300 cm^{-1}, although the bandwidth is much narrow at lower wavenumbers. To minimize an energy loss of the infrared beam and an overwhelming spectral interference from water vapor absorption, 95% of the infrared beam path was purged with dry nitrogen gas (in-house N_2 vapor above a liquid nitrogen reservoir). For the visible and infrared beams, 300 and ~10 μJ of energy was utilized, respectively.

Polarization combinations of ssp (s-SFG; s-visible; p-infrared) were used, and the incident angles of the visible and infrared beams were 53 and 70° with respect to the surface normal, respectively. To arrive at the final VSFG spectra presentation, background-subtracted VSFG spectra were normalized against the broadband infrared beam energy profile using a nonresonant VSFG spectrum from a GaAs crystal (Lambda Precision Optics, Inc.). The purpose of doing the normalization is to eliminate the spectral distortion caused by the infrared beam energy

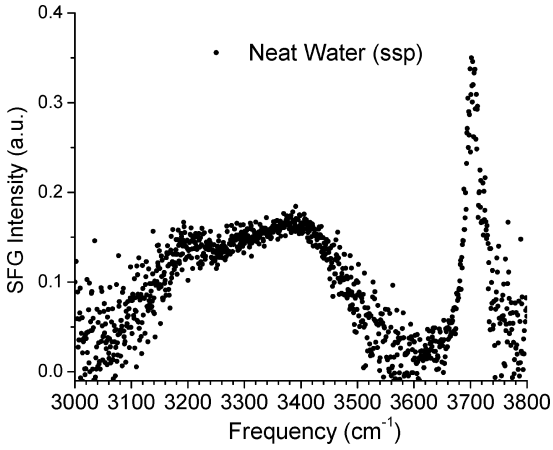

Figure 1. ssp VSFG spectrum of neat water at 23 °C in O−H stretching region. (All figure intensities can be compared against each other using the plotted SFG intensity *y*-axis scales.)

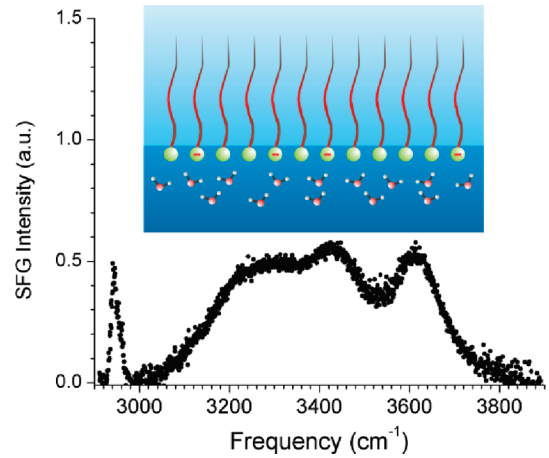

Figure 2. ssp VSFG spectrum of the PA monolayer on water at 23 °C in O−H stretching region.

distribution associated with each frequency in the spectral region of interest. Spectral calibration of VSFG peak positions was completed by comparing the polystyrene absorption bands obtained from a nonresonant GaAs spectrum to reference FTIR spectra. By doing this, the VSFG peak positions reported are accurate to 1 cm^{-1}. PA spectra on salt solutions (Figures 3 and 4) are shown beginning at 3000 cm^{-1}; however, the $\nu_{FR}CH_3$ band was observed at 2940 cm^{-1} for all of these spectra, ruling out any question about the PA remaining surface active upon deprotonation and binding. Spectral assignments are discussed in terms of the apparent peak positions since only PS-VSFG spectra can determine the absolute phase of the broad bands in the hydrogen bonded stretch region.[59]

All spectral intensities can be directly compared using the *y*-axis units from all figures. Spectra shown here (in addition to reproduced spectra) were obtained under the same SFG conditions over a period of days of constant energy and alignment, and spectral reference systems were attained between sample acquisitions to verify.

Results and Discussion

Of primary focus in this study is the interfacial hydrogen-bonding network that exists uniquely between a PA Langmuir monolayer and surface water molecules at the air/liquid interface. More importantly, divalent cation binding to the PA headgroup and its direct effect on the surrounding hydrogen-bonding network were systematically investigated. In the following, vibrational spectral evidence that reveals the nature of this interfacial hydrogen-bonding network is presented.

As a reference, a neat water VSFG spectrum is shown in Figure 1. This spectrum in the O−H stretching region (3000−3900 cm^{-1}) reveals two apparent broad bands and one distinctly narrow vibrational band that are attributed to the predominant hydrogen-bonded water structures at the air/liquid interface. In the order of increasing vibrational frequency, or decreasing hydrogen-bonding strength, the regions are identified with approximate spectral positions of 3200 and 3400 cm^{-1} with a much sharper peak at 3700 cm^{-1}. Even though a definitive assignment is still missing due to the collective nature of potentially inter- and intramolecular interactions of O−H oscillators both in the bulk and at the interface, one may generally agree that the low frequency band (∼3200 cm^{-1}) represents a more ordered hydrogen-bonding structure than that of the midfrequency band (∼3400 cm^{-1}). In practice, these are commonly assigned to the symmetrically and the asymmetrically hydrogen-bonded water molecules, respectively.[60] In addition, the ∼3700 cm^{-1} sharp band, generally known as the dangling or free O−H band, is assigned to the uncoupled O−H oscillators that protrude into the air phase, leaving the other halves in water to participate in the hydrogen-bonding network at the interface. Moreover, according to the recent phase study published by Shen's group,[61] the former two broad bands are opposite in phase, that is, the average polar orientation of O−H oscillators are pointing opposite against each other, that is, the 3200 and 3400 cm^{-1} band water molecules point their hydrogens toward and away from the surface plane, respectively. These phase assignments and measurements have been confirmed by Tahara and co-workers and by Allen and co-workers.[42,43]

The interfacial hydrogen-bonding network is susceptible to perturbations. According to the findings by Miranda et al.,[52] considerable disruption occurs to the hydrogen-bonding network of the interfacial water molecules underneath a neutral fatty acid layer; but a charged surface, as a result of the dissociation of fatty acid headgroups at pH greater than 7.0, reestablishes the hydrogen-bonding network due to charge-dipole interactions, which are also termed as the polar ordering effect of the surface negative electric field on the interfacial water molecules. Accordingly, Figure 2 shows an ssp VSFG spectrum of the PA Langmuir monolayer-covered water surface at a near neutral pH (∼ 6.0). Four vibrational bands with enhanced intensities are observed across the spectrum. In the order of increasing frequency, these bands are separately located at ∼2940, ∼3250, ∼3400, and ∼3600 cm^{-1}. These spectral features are closely in agreement with the reported VSFG spectra obtained by Miranda in a similar study.[52] First, the appearance of the ∼2940 cm^{-1} ($\nu_{FR}CH_3$) affirms the presence of the PA monolayer at the interface. Because of the limited range of the infrared profile (2900−3900 cm^{-1}) used, we were not probing the symmetric modes of C−H stretches of the acyl chains. Second, in comparison, the two bands with intermediate frequencies in the PA−water spectrum show similar spectral features with respect to the hydrogen-bonding continuum as appeared in the neat water spectrum of Figure 1; therefore, these are attributed to the O−H oscillators that are associated with the interfacial hydrogen-bonded water molecules. This assignment has been adopted in past VSFG studies by many groups. At the highest frequencies, the ∼3600 cm^{-1} band is relatively strong in intensity. This mode has been previously ascribed to the

hydrogen-bonded OH oscillators that exist uniquely between surface water molecules and the fatty acid headgroups by Miranda et al.;[52] in addition, this band has also been identified in IRRAS studies of similar monolayer systems at the air/liquid interface.[39] In addition, we further confirm this assignment in recent work.[58] By appearing at the blue side of the hydrogen-bonding network, this hydrogen bond is relatively weaker than those existing among interfacial water molecules participating in the hydrogen-bonding continuum.

In looking at the overall intensity enhancement in the PA−water spectrum relative to the neat water spectrum, surface field effects can best explain the ordering of hydrogen-bonded water molecules at the interface (Debye length of ∼300 nm). Our most recent PS-VSFG studies showed that all (3000−3700 cm^{-1}) interfacial water molecules point their hydrogens on average toward the surface plane as shown in the schematic in the inset of Figure 2. At pH 6.0, the majority of the PA headgroups is protonated (99.8%) at the surface according to the reported surface pK_a (∼8.7) of long-chain fatty acids.[62,63] This value has also been confirmed by our pH study as evidenced by the spectral data acquired with respect to the normal modes of carboxylic and carboxylate groups (1200−1500 cm^{-1}); however, small degrees of deprotonation still exist according to the small reduction of intensities of carboxylic modes (νC−O and νC═O) as pH increases from ∼2.0 to 6.0.[64] Because of the presence of negative charges as the result of dissociation of PA headgroups, the surface field effect is pronounced, as revealed by the enhanced spectral response from the PA and water interface in relation to the neat water surface. This effect has also been attributed to the $\chi^{(3)}$ effect.[65,66]

Ionic perturbations on the interfacial hydrogen-bonding network are apparent in the presence of ionic species in the bulk. Figure 3A exhibits ssp VSFG spectra of PA monolayers spread over Mg^{2+} aqueous solution surfaces at four different bulk concentrations (0.1, 0.3, 1.5, and 2.6 M). The most pronounced effect with respect to the spectrum of PA on the water surface is the overall decrease of band intensities as the bulk concentration is increased from 0.1 to 1.5 M, and then is followed by the reemergence of both ∼3200 and ∼3400 cm^{-1} bands at 2.6 M. Even though intensity attenuation is not overwhelmingly significant at 0.1 M, the reductions of ∼3200 and ∼3600 cm^{-1} intensities are noticeable, and more so at 0.3 and 1.5 M with additional decrease of the ∼3450 cm^{-1} band. Considering the ∼3600 cm^{-1} band alone, its progressive intensity attenuation during the concentration increase is consistent with the spectral evidence observed in other spectral regions (νC═O and $\nu_s COO^-$).[64] This trend affirms the basic principle that cation binding to the carboxylic headgroup directly correlates to the cation concentration in the bulk. Even though this mechanism is insignificant at low concentrations, at higher concentrations it can become much more enhanced. On the basis of the obtained spectral evidence, Mg^{2+} binds to COO^- but the binding strength is relatively weak. At 0.1 M, the degree of deprotonation of the PA headgroups is insignificant due to weak binding strength and insufficient numbers of Mg^{2+}, but at a higher concentration of Mg^{2+} (0.3 M), a small population of bidentate ionic complexes start to evolve.[64] As a consequence, the 3600 cm^{-1} band starts to attenuate as a sign of decreasing numbers of protonated headgroups.

As a general rule, a decrease of the ∼3200 cm^{-1} band may reflect a possible disruption of the symmetrical hydrogen-bonding network and an increase of ∼3400 cm^{-1} band may reveal an augment of the asymmetrically hydrogen-bonded, or solvation shell, water structure. Therefore, the reduction of the

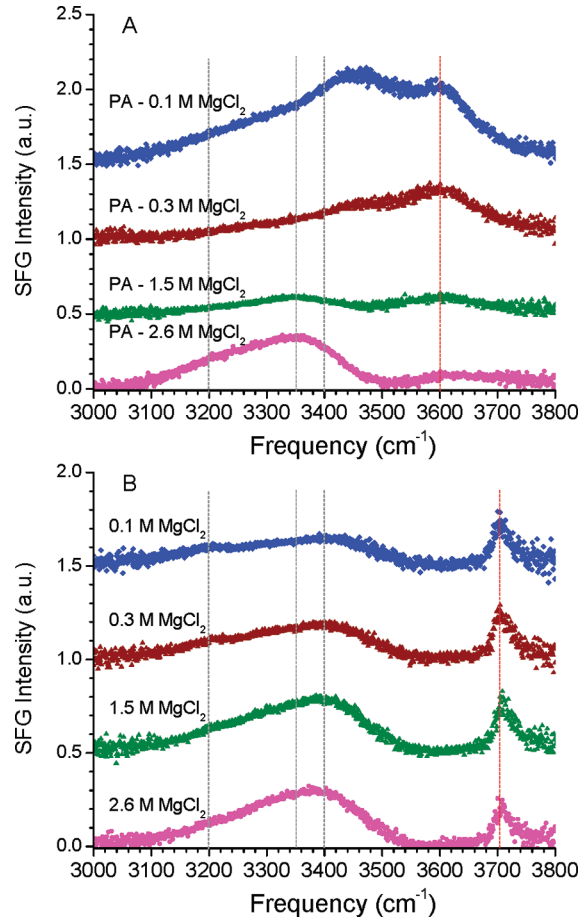

Figure 3. ssp VSFG spectra in O−H stretching region. (A) PA monolayers on aqueous $MgCl_2$ solutions (0.1, 0.3, 1.5, and 2.6 M) at 23 °C; (B) neat (no monolayer) $MgCl_2$ solutions (0.1, 0.3, 1.5, and 2.6 M) at 23 °C.

∼3200 cm^{-1} band as shown in Figure 3A can be attributed to the disruption of the symmetrically hydrogen-bonding network. However, the ∼3450 cm^{-1} band does not faithfully obey the similar trend demonstrated by the ∼3200 cm^{-1} band. At first, there is no apparent reduction of this intensity at 0.1 M Mg^{2+} in comparison to Figure 2. Then, significant reductions take place at 0.3 and 1.5 M and later being followed by the reappearance of its intensity at 3200 and 3350 cm^{-1}. To correctly interpret these unique physical trends observed in the spectra, the underlying ionic binding mechanism is considered to be the primary factor dictating the spectral outcome.

Cation binding to COO^- has an equivalent effect of surface charge neutralization, or charge screening as demonstrated by charged double layers of the Guoy-Chapman model;[67] therefore, more binding events tend to produce more of this effect. Additionally informative, from calculation at pH of 6 a PA monolayer on neat water has a Debye length of ∼300 nm, and upon addition of 0.1 M divalent salts (e.g., $MgCl_2$) that length shortens considerably to less than 1 nm. As a consequence of charge neutralization, the decharging mechanism directly affects the signal response of the ∼3200 and ∼3450 cm^{-1} bands from the hydrogen-bonding network; in particular, the most pronounced effect is the attenuation of band intensities as the zero-point-charge (ZPC) is approached at the interface. For instance, the same effect has been separately demonstrated in studies of fatty acid salt adsorption on the CaF_2 surface and hydrophobic adsorption on a modified silica surface at the liquid−solid interface by Richmond and Shen, respectively.[53,54]

Hence, it is consistent to observe a relatively small reduction of the ~3450 cm^{-1} band at 0.1 M Mg^{2+}, and yet large reductions at 0.3 and 1.5 M with respect to the spectrum obtained from the PA monolayer on the water surface as seen in Figure 3A. Mg^{2+} is strongly hydrated and it is energetically unfavorable to remove its solvation shell water molecules before making a bound ionic complex with COO^-, as the order of solvation energy of Mg^{2+} is large ($Mg^{2+} > Ca^{2+} \gg RCOOH \gg H_2O$). This has been inferred for the Mg^{2+}, carboxylate, and water system by ab initio calculations.[68] At 0.1 M, the formation of bound ionic complexes (Mg^{2+}/COO^-) is unlikely in which case surface charge neutralization is insignificant because only a small fraction of Mg^{2+} is interacting with COO^-, and furthermore the majority of these interacting Mg^{2+} has its solvation shell intact, or mostly so. As a result, the overall spectral intensity, especially the ~3450 cm^{-1} band for the 0.1 M solution in Figure 3A, remains as strong as that of the spectrum corresponding to the PA monolayer on water in Figure 2 owing to the surface field effect. Nevertheless, the progressive reductions of the overall spectral intensity at 0.3 and 1.5 M are indicative of surface charge neutralization as formation of bidentate ionic complexes is considerably accentuated. (Additional evidence is from the significant increase of the $\upsilon_s COO^-$ intensity at 1475 cm^{-1} at 1.5 M Mg^{2+} (data not shown).) More importantly, the noticeable resurgence of the ~3350 cm^{-1} band at 1.5 M Mg^{2+} clearly marks a critical transition in the interfacial water structure, at which spectral characteristics of the neat Mg^{2+} solution interface start to emerge in the hydrogen-bonding continuum (3000−3600 cm^{-1}). This spectral data will be discussed below. By implication, we suggest that at the 1.5 M transition concentration, the primary contributions to the hydrogen-bonding network consist of water molecules participating in the solvation shells of inorganic ions and the undissociated PA headgroups.

As surface charge neutralization surpasses the PZC, the trend is reversed. At 2.6 M, the 3600 cm^{-1} band becomes significantly reduced compared to that of lower concentrations. Such a reduced intensity is accompanied by an increasing presence of bound ionic complexes at the interface since this band signifies the presence of deprotonated headgroups. After surface charge neutralization as a result of forming bound ionic complexes in the presence of excess Mg^{2+}, the interfacial hydrogen-bonded water molecules reorganize and revert to the hydrogen-bonding structure as that of the neat Mg^{2+} solution interface shown in Figure 3B. This suggests that the water structure underneath the PA Langmuir monolayer at concentrated Mg^{2+} conditions exhibits the similar hydrogen-bonding network as those shown in neat salt solutions. The only exception is that the original dangling O−H band (3700 cm^{-1}) completely disappears while the solvated carboxylic O−H band becomes dominant. Unlike adsorption studies at the solid/liquid interface, the reversal effect observed in this study is not in terms of recharging the surface by forming multilayer adsorptions. If that was the case, much more enhanced spectral intensity would reappear across the spectrum as that in Figure 2; however, that is not so. Therefore, the unique physical picture can be described as the interfacial hydrogen-bonded water molecules surrounding the cation-complexed PA headgroups reorganize to near to the original hydrogen-bonding structure as appears in the neat Mg^{2+} solution interfaces when a significant fraction of the headgroups becomes bound with Mg^{2+}, for example, at concentrations at and above 1.5 M Mg^{2+}.

Even more clearly observed in Figure 4A, ssp VSFG spectra of the PA monolayers spread over Ca^{2+} aqueous solution surfaces with corresponding bulk concentrations at 0.1, 0.3, and 1.8 M reveal suppression of the surface charge through cation complexation with increasing salt concentration. According to Figure 4A, it is evident that the overall signal strength is much weaker relative to that in Figure 3A at low concentrations (0.1 and 0.3 M). Likewise, at a concentrated condition (1.8 M), a spectrum similar to that of neat Ca^{2+} also reemerges, except the disappearance of the dangling O−H band relative to the neat salt solutions shown in Figure 4B. By comparison, this is consistent with the spectral data exhibited in Figure 3. Ca^{2+} and Mg^{2+} tend to behave similarly when considering their influence on the interfacial hydrogen-bonding network at high concentrations. More or less they share some common influence as would be suggested from Debye length calculations. But the most distinct variation is the complete disappearance of the ~3600 cm^{-1} band at 1.8 M Ca^{2+}. This is indicative of complete deprotonation that results in the PA headgroups due to Ca^{2+} binding, which is much stronger than Mg^{2+}, which is not suggested through Debye length calculation.

In general, this deprotonation effect also appears as a function of Ca^{2+} concentration since the degree of deprotonation is progressively enhanced as Ca^{2+} concentration increases, as evidenced in the spectra. The disappearance of the 3600 cm^{-1} band also agrees consistently with the spectral evidence presented in $\nu_s COO^-$ and $\nu C{=}O$ spectral regions.[64] Collectively, these cations manifest a complete deprotonation of the PA

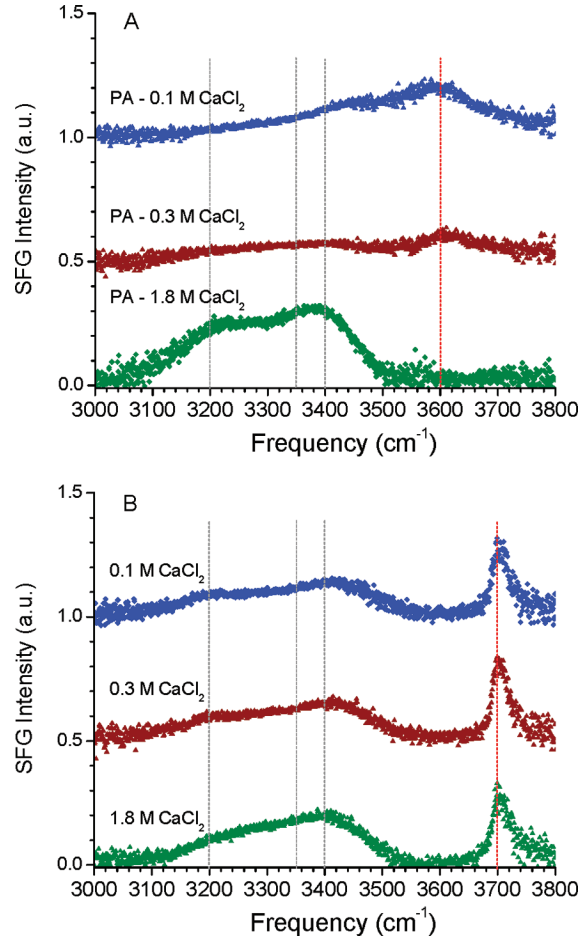

Figure 4. ssp VSFG spectra in O−H stretching region. (A) PA monolayers on aqueous $CaCl_2$ solutions (0.1, 0.3, and 1.8 M) at 23 °C; (B) neat (no monolayer) $CaCl_2$ solutions (0.1, 0.3, and 1.8 M) at 23 °C.

headgroups due to the formation of bound ionic complexes. Taking into account the considerable attenuation of the ~3200 and ~3450 cm^{-1} bands in the spectra associated with 0.1 and 0.3 M Ca^{2+}, strong binding affinity of Ca^{2+} to the PA monolayer neutralizes the surface charge more efficiently. For instance, this effect already becomes dominant at 0.3 M Ca^{2+} as compared to that of 1.5 M Mg^{2+}. Thus, it supports the assertion that Ca^{2+} interacts much more strongly with COO^- than Mg^{2+} at the air/liquid interface. This may also explain why Mg^{2+} and Ca^{2+} compression isotherms are distinctively different in terms of charge screening ability of cations considered.[64] In summary, Ca^{2+} has stronger binding affinity toward the PA headgroups than Mg^{2+} so that it is capable of neutralizing surface charge at a much lower concentration than Mg^{2+}. This is further evidenced by spectral results that obey surface charge neutralization effects on the hydrogen-bonding network at the air/liquid interface.

Conclusions

In this study, we investigated the interfacial hydrogen-bonding network that uniquely exists in between the PA Langmuir monolayer and the underneath surface water molecules, and more importantly, we identified that cation binding of Mg^{2+} and Ca^{2+} to the PA headgroup has considerable impact on the hydrogen-bonding network, which is not elucidated through calculation of the Debye length. A significant enhancement of the overall spectral intensity appears for the PA monolayer at near neutral pH. Polar ordering of the interfacial water molecules under the influence of the surface field of the dissociated PA headgroups is observed. We conclude that only a small fraction of negative charges can induce considerable polar ordering in the interfacial water molecules. We found Ca^{2+} has a much greater impact on the interfacial hydrogen-bonding network than Mg^{2+} because Ca^{2+} has a much greater binding affinity relative to Mg^{2+}. Therefore, the transition point at which surface water structures reorganize occurs at a much lower concentration for Ca^{2+} as compared with Mg^{2+}. More importantly, at concentrated conditions the already disrupted hydrogen-bonding network structure reorganizes and reverts to its original hydrogen-bonding network as that which appeared at the neat salt solution surface.

As a final note, an in-depth understanding of the dynamic nature of the interfacial hydrogen-bonding network that exists beneath the PA Langmuir monolayer in the presence divalent cations such as Mg^{2+} and Ca^{2+} is of great importance in making predictions regarding surface phenomena that are commonly found at both biological and atmospheric aerosol interfaces.

Acknowledgment. We thank the National Science Foundation, NSF-CHE, for funding this work.

References and Notes

(1) *Water and the Cell*; Pollack, G. H., Cameron, I. L., Wheatley, D. N., Eds.; Springer Netherlands: Dordrecht, 2006.
(2) *Protein - solvent interactions*; Gregory, R. B., Ed.; Marcel Dekker Inc.: New York, 1995.
(3) Tarek, M.; Tobias, D. J. *Phys. Rev. Lett.* **2002**, *88*, 4.
(4) *Nanobiotechnology of Biomimetic Membranes*; Martin, D. K., Ed.; Springer: New York, 2007.
(5) Mmereki, B. T.; Donaldson, D. J.; Gilman, J. B.; Eliason, T. L.; Vaida, V. *Atmos. Environ.* **2004**, *38*, 6091.
(6) Voss, L. F.; Bazerbashi, M. F.; Beekman, C. P.; Hadad, C. M.; Allen, H. C. *J. Geophys. Res., (Atmos.)* **2007**, *112*, 9.
(7) Kaganer, V. M.; Mohwald, H.; Dutta, P. *Rev. Mod. Phys.* **1999**, *71*, 779.
(8) Nylander, T.; Campbell, R. A.; Vandoolaeghe, P.; Cardenas, M.; Linse, P.; Rennie, A. R. *Biointerphases* **2008**, *3*, FB64.
(9) Liu, J.; Conboy, J. C. *J. Phys. Chem. C* **2007**, *111*, 8988.
(10) Auguste, D. T.; Kirkwood, J.; Kohn, J.; Fuller, G. G.; Prud'homme, R. K. *Langmuir* **2008**, *24*, 4056.
(11) Gericke, A.; Huhnerfuss, H. *Thin Solid Films* **1994**, *245*, 74.
(12) Liu, H. J.; Du, X. Z.; Li, Y. *J. Phys. Chem. C* **2007**, *111*, 17025.
(13) Ma, G.; Allen, H. C. *Langmuir* **2007**, *23*, 589.
(14) Petrash, S.; Cregger, T.; Zhao, B.; Pokidysheva, E.; Foster, M. D.; Brittain, W. J.; Sevastianov, V.; Majkrzak, C. F. *Langmuir* **2001**, *17*, 7645.
(15) Aston, M. S. *Chem. Soc. Rev.* **1993**, *22*, 67.
(16) Yazdanian, M.; Yu, H.; Zografi, G. *Langmuir* **1990**, *6*, 1093.
(17) Mobius, D. *Curr. Opin. Colloid Interface Sci.* **1998**, *3*, 137.
(18) McConnell, H. M. *Annu. Rev. Phys. Chem.* **1991**, *42*, 171.
(19) Mendelsohn, R.; Brauner, J. W.; Gericke, A. *Annu. Rev. Phys. Chem.* **1995**, *46*, 305.
(20) Vogel, V.; Mullin, C. S.; Shen, Y. R. *Langmuir* **1991**, *7*, 1222.
(21) Zhuang, X. W.; Marrucci, L.; Shen, Y. R. *Phys. Rev. Lett.* **1994**, *73*, 1513.
(22) Zhang, D.; Gutow, J.; Eisenthal, K. B. *J. Phys. Chem.* **1994**, *98*, 13729.
(23) Du, Q.; Superfine, R.; Freysz, E.; Shen, Y. R. *Phys. Rev. Lett.* **1993**, *70*, 2313.
(24) Baldelli, S.; Schnitzer, C.; Shultz, M. J.; Campbell, D. J. *J. Phys. Chem. B* **1997**, *101*, 10435.
(25) Gragson, D. E.; McCarty, B. M.; Richmond, G. L. *J. Am. Chem. Soc.* **1997**, *119*, 6144.
(26) Kim, J.; Cremer, P. S. *J. Am. Chem. Soc.* **2000**, *122*, 12371.
(27) Ye, S.; Nihonyanagi, S.; Uosaki, K. *Phys. Chem. Chem. Phys.* **2001**, *3*, 3463.
(28) Liu, D.; Ma, G.; Levering, L. M.; Allen, H. C. *J. Phys. Chem. B* **2004**, *108*, 2252.
(29) Fitchett, B. D.; Conboy, J. C. *J. Phys. Chem. B* **2004**, *108*, 20255.
(30) Tyrode, E.; Johnson, C. M.; Baldelli, S.; Leygraf, C.; Rutland, M. W. *J. Phy. Chem. B* **2005**, *109*, 329.
(31) Bordenyuk, A. N.; Benderskii, A. V. *J. Chem. Phys.* **2005**, *122*, 134713.
(32) Nickolov, Z. S.; Britt, D. W.; Miller, J. D. *J. Phys. Chem. B* **2006**, *110*, 15506.
(33) Nishida, T.; Johnson, C. M.; Holman, J.; Osawa, M.; Davies, P. B.; Ye, S. *Phys. Rev. Lett.* **2006**, *96*, 4.
(34) Sovago, M.; Campen, R.; Wurpel, G.; uuml; ller, M.; Bakker, H.; Bonn, M. *Phys. Rev. Lett.* **2008**, *100*, 173901.
(35) Jena, K. C.; Hore, D. K. *J. Phys. Chem. C* **2009**, *113*, 15364.
(36) Yang, Z.; Li, Q. F.; Chou, K. C. *J. Phys. Chem. C* **2009**, *113*, 8201.
(37) Kmetko, J.; Datta, A.; Evmenenko, G.; Dutta, P. *J. Phys. Chem. B* **2001**, *105*, 10818.
(38) Schlossman, M. L.; Tikhonov, A. M. *Annu. Rev. Phys. Chem.* **2008**, *59*, 153.
(39) Liu, H. J.; Zheng, H. F.; Miao, W. G.; Du, X. Z. *Langmuir* **2009**, *25*, 2941.
(40) Ivanova, A.; Tadjer, A.; Tyutyulkov, N.; Radoev, B. *J. Phys. Chem. A* **2005**, *109*, 1692.
(41) Ostroverkhov, V.; Waychunas, G. A.; Shen, Y. R. *Phys. Rev. Lett.* **2005**, *94*, 4.
(42) Nihonyanagi, S.; Yamaguchi, S.; Tahara, T. *J. Chem. Phys.* **2009**, *130*, 5.
(43) Chen, X.; Hua, W.; Huang, Z.; Allen, H. C. *J. Am. Chem. Soc.* **2010**, *132*, 11336.
(44) Baldelli, S.; Schnitzer, C.; Shultz, M. J.; Campbell, D. J. *Chem. Phys. Lett.* **1998**, *287*, 143.
(45) Baldelli, S.; Schnitzer, C.; Shultz, M. J. *Chem. Phys. Lett.* **1999**, *302*, 157.
(46) Raymond, E. A.; Richmond, G. L. *J. Phys. Chem. B* **2004**, *108*, 5051.
(47) Gopalakrishnan, S.; Jungwirth, P.; Tobias, D. J.; Allen, H. C. *J. Phys. Chem. B* **2005**, *109*, 8861.
(48) Xu, M.; Spinney, R.; Allen, H. C. *J. Phys. Chem. B* **2009**, *113*, 4102.
(49) Bian, H. T.; Feng, R. R.; Guo, Y.; Wang, H. F. *J. Chem. Phys.* **2009**, *130*, 11.
(50) Tian, C. S.; Ji, N.; Waychunas, G. A.; Shen, Y. R. *J. Am. Chem. Soc.* **2008**, *130*, 13033.
(51) Gurau, M. C.; Kim, G.; Lim, S. M.; Albertorio, F.; Fleisher, H. C.; Cremer, P. S. *ChemPhysChem* **2003**, *4*, 1231.
(52) Miranda, P. B.; Du, Q.; Shen, Y. R. *Chem. Phys. Lett.* **1998**, *286*, 1.
(53) Becraft, K. A.; Richmond, G. L. *J. Phys. Chem. B* **2005**, *109*, 5108.
(54) Tian, C. S.; Shen, Y. R. *Proc. Natl. Acad. Sci. U.S.A. U.S.A.* **2009**, *106*, 15148.
(55) Finlayson, A. C. *J. Chem. Educ.* **1992**, *69*, 559.
(56) Hommel, E. L.; Allen, H. C. *Anal. Sci.* **2001**, *17*, 137.
(57) Ma, G.; Allen, H. C. *J. Phys. Chem. B* **2003**, *107*, 6343.
(58) Tang, C. Y.; Allen, H. C. *J. Phys. Chem. A* **2009**, *113*, 7383.
(59) Shen, Y. R.; Ostroverkhov, V. *Chem. Rev.* **2006**, *106*, 1140.
(60) Moore, F. G.; Richmond, G. L. *Acc. Chem. Res.* **2008**, *41*, 739.

(61) Tian, C. S.; Shen, Y. R. *J. Am. Chem. Soc.* **2009**, *131*, 2790.
(62) Gershevitz, O.; Sukenik, C. N. *J. Am. Chem. Soc.* **2004**, *126*, 482.
(63) Gomez-Fernandez, J. C.; Villalain, J. *Chem. Phys. Lipids* **1998**, *96*, 41.
(64) Tang, C. Y.; Huang, Z.; Allen, H. C. *J. Phys. Chem. B*, published online Nov 9, http://dx.doi.org/10.1021/jp105472e.
(65) Zhao, X. L.; Subrahmanyan, S.; Eisenthal, K. B. *Chem. Phys. Lett.* **1990**, *171*, 558.
(66) Geiger, F. M. *Annu. Rev. Phys. Chem.* **2009**, *60*, 61.
(67) Adamson, A. W.; Gast, A. P. *Physical chemistry of surfaces*; Wiley: New York, 1997.
(68) Katz, A. K.; Glusker, J. P.; Markham, G. D.; Bock, C. W. *J. Phys. Chem. B* **1998**, *102*, 6342.

JP1062447